Journal of Solid State Chemistry **168,** 28–33 (2002)
doi:10.1006/jssc.2002.9671

The Ternary Gallide CeNiGa: Polymorphism and Hydrogen Absorption

B. Chevalier,[1] J.-L. Bobet, E. Gaudin, M. Pasturel, and J. Etourneau

Institut de Chimie de la Matière Condensée de Bordeaux (ICMCB), CNRS [UPR 9048], Université Bordeaux I, Avenue du Docteur A. Schweitzer, 33608 Pessac Cedex, France

Received February 26, 2002; in revised form May 6, 2002; accepted May 28, 2002

The ternary gallide CeNiGa presents a crystallographic transformation with temperature. The crystal structure of the high-temperature form (HTF), determined for the first time by X-ray diffraction on a single crystal, is orthorhombic TiNiSi-type, whereas the low-temperature form (LTF) adopts the hexagonal ZrNiAl-type. Electrical resistivity and magnetization measurements reveal that both (LTF) and (HTF) CeNiGa are classified as intermediate valence compounds, but their Kondo temperatures T_K are strongly different; $T_K \gg 300$ K and $T_K \cong 95(5)$ K for (LTF) and (HTF), respectively. Both forms react with hydrogen at room temperature and form the hydride $CeNiGaH_{1.1(1)}$ which crystallizes in the hexagonal AlB_2-type with lattice parameters $a = 4.239(4)$ Å and $c = 4.258(5)$ Å. Hydrogenation also induces a valence transition for cerium from the intermediate valence state (CeNiGa) to a purely trivalent state ($CeNiGaH_{1.1(1)}$). This behavior is correlated to an increase of the unit cell volume after hydrogenation and is compared to that observed previously for $CeNiAlH_{1.93}$.

Key Words: **cerium compounds; X-ray diffraction; intermediate valence; hydrogenation; magnetism.**

1. INTRODUCTION

The intermetallic compounds CeNiAl and CeNiIn which crystallize in the hexagonal ZrNiAl-type structure, absorb hydrogen at room temperature (1–4). For instance, the hydrides $CeNiAlH_{1.93}$ and $CeNiInH_{1.6–1.8}$ are obtained after exposing the starting samples to a hydrogen pressure of 1–10 MPa (1, 2, 4). For CeNiAl, the absorption of hydrogen induces a structural transition from hexagonal ZrNiAl-type to hexagonal AlB_2-type (1). On the contrary, the initial ZrNiAl-type is preserved after hydrogen insertion into CeNiIn and only a pronounced anisotropic expansion of the unit cell is evidenced (3, 4). Steric considerations can be proposed in order to explain these structural changes. As the atomic radius of aluminum ($r_{Al} = 1.43$ Å) is smaller than that of indium ($r_{In} = 1.66$ Å), the unit cell volume of CeNiAl ($V_m = 169.50$ Å^3) (1) is smaller than that of CeNiIn ($V_m = 194.73$ Å^3) (4). Accordingly, the tetrahedral interstices (Ce_3Ni, Ce_2Ni_2…) identified as possible sites for insertions of H-atom are too small in CeNiAl (4), but can be large enough in CeNiIn. Only sites having a radius exceeding 0.4 Å can be considered for hydrogen insertion.

Moreover, hydrogenation of CeNiAl and CeNiIn induces a valence transition for cerium. These compounds are considered as intermediate valence materials having a very high Kondo temperature (5). On the contrary, the magnetic susceptibility measurements revealed a trivalent state for cerium in $CeNiAlH_{1.93}$ (1) and $CeNiInH_{1.6}$ (3). The valence transition from intermediate to Ce^{3+} state results from the increase of the interatomic distances between the Ce-atom and its ligands after hydrogenation. In these conditions, the localization of the Ce(4*f*)-electrons is greater. The hydrogenation of the cerium-based intermetallics is of great interest in the study of the magnetic instabilities resulting from the hybridization of the Ce(4*f*)-electrons with those of the conduction band.

In order to obtain more information on the crystallographic factors governing the structural properties of the hydrides $CeNiXH_Y$ (X = p elements), the hydrogen absorption properties of CeNiGa have been studied. It is important to note that the atomic radius of gallium ($r_{Ga} = 1.41$ Å) is smaller than those of Al- or In-atoms. Previous studies devoted to this ternary gallide indicate a polymorphism transition around 973 K: the low-temperature form (LTF) adopts, as do CeNiAl and CeNiIn, the hexagonal ZrNiAl-type structure, whereas the crystal structure of the high-temperature form (HTF) is unknown (6, 7). In this paper, the structural, electrical and magnetic properties of the two CeNiGa forms are reported. Also, the synthesis of the hydride $CeNiGaH_X$ and its magnetic properties are discussed in relation with those determined previously for $CeNiAlH_Y$ and $CeNiInH_Y$.

[1] To whom correspondence should be addressed. Fax: 33-5-56842761. E-mail: chevalie@icmcb.u-bordeaux.fr.

0022-4596/02 $35.00

2. EXPERIMENTAL PROCEDURES

The sample CeNiGa was synthesized by arc-melting a stoichiometric mixture of pure elements (purity above 99.9%) in a high-purity argon atmosphere. Then, the sample was turned and remelted several times to ensure homogeneity. The weight loss during the arc-melting process was less than 0.5 wt%. Annealing was done for 1 month by enclosing the sample in evacuated quartz tubes. One half of the ingot was annealed at 873 K and the other half at 1073 K followed by a quick cooling at room temperature.

Hydrogen absorption experiments were performed using the apparatus described previously (8). An ingot of an annealed sample was heated under vacuum at 473 K for 12 h and then exposed to hydrogen gas at room temperature and 5 MPa. The amount of H-absorption was determined volumetrically by monitoring pressure changes in a calibrated volume.

X-ray powder diffraction with the use of a Philips 1050-diffractometer (Cu$K\alpha$ radiation) was applied for the characterization of the structural type and for the phase identification of the samples. The unit cell parameters were determined by a least-squares refinement method using silicon (5 N) as an internal standard. The crystal structures of LTF CeNiGa and CeNiGaH_Y were refined by the Rietveld profile method (9). The refinement of the crystal structure of the sample annealed at 1073 K (HTF) was performed using a tiny single crystal isolated from the sample by mechanical fragmentation. The data collection was carried out on an Enraf–Nonius Kappa CCD diffractometer using Mo$K\alpha$ radiation. Data processing was performed with the Jana 2000 software (10). A Gaussian-type absorption correction was applied and the shape was estimated with the video microscope of the Kappa CCD.

Magnetization measurements were performed using a Superconducting QUantum Interference Device (SQUID) magnetometer in the temperature range 1.8–300 K and applied fields up to 5 T. Electrical resistivity was determined above 4.2 K on a polycrystalline sample using standard dc four-probe measurements.

3. RESULTS AND DISCUSSION

3.1. Structural Properties

3.1.1. The Two CeNiGa Temperature Forms

Figure 1 presents the X-ray powder patterns of CeNiGa obtained after annealing at 873 or 1073 K. The patterns are different, showing that this ternary gallide exhibits crystallographic dimorphism.

X-ray powder diffraction performed on CeNiGa annealed at 873 K (LTF) reveals only the peaks corresponding to the expected hexagonal ZrNiAl structure type. The refined unit cell parameters $a = 6.9421(5)$ Å and $c = 3.9762(5)$ Å are in agreement with those determined previously (6, 7).

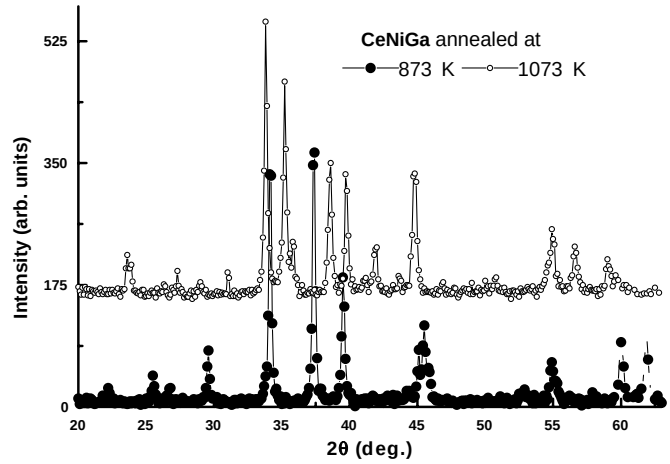

FIG. 1. X-ray powder pattern of CeNiGa annealed at 873 and 1073 K.

The structure of CeNiGa annealed at 1073 K (HTF) has been determined from single-crystal X-ray data. The extinction conditions observed for both data sets agree with the *Pnma* space group (No. 62) which was already used for the refinement of the ternary gallides *RE*NiGa with *RE* = Pr → Lu (6) (for data collection details, see Table 1). The atomic positions were found by direct methods using SHELXS-97 software (11). With the resulting atomic positions and isotropic atomic displacement parameters (Table 2), the residual factors converged to $R(F) = 0.0824$ and $wR(F^2) = 0.1598$. With anisotropic displacement parameters (Table 3) and secondary extinction (12), the final residual factors took the value $R(F) = 0.0447$ and $wR(F^2) = 0.1024$ for 20 refined parameters and 291 observed reflections.

HTF CeNiGa adopts the orthorhombic TiNiSi-type structure like the other rare-earth-based equiatomic ternary gallides *RE*NiGa (6). But CeNiGa is the only compound of this series presenting two crystal structures versus temperature. Certainly, the possibility of Ce-species to exhibit an intermediate valence state plays an important role in the structural properties of CeNiGa. The unit cell volume of CeNiGa (HTF), equal to 229.2 Å^3 (Table 1), is slightly smaller than that observed for PrNiGa (231.3 Å^3). Other interesting observation concerns the unit cell parameters of CeNiGa (HTF); as for PrNiGa (6), the *a*-parameter is greater than the *c*-parameter (Table 1). This characteristic is exceptional among the series of the ternary gallides *RE*NiGa since the ratio c/a is greater than 1 excepted for *RE* = Ce and Pr. According to statistics available on the compounds crystallizing with the TiNiSi-type structure, it is well established that the positional parameters of the

TABLE 1
Crystallographic Data and Structure Refinement for CeNiGa (HTF)

Crystal data	
Chemical formula	CeNiGa
Chemical formula weight ($g\,mol^{-1}$)	268.5
Temperature	293 K
Crystal system	Orthorhombic
Space group	*Pnma* (no. 62)
Unit cell dimension	$a = 7.4477(15)$ Å $b = 4.5308(9)$ Å $c = 6.7923(14)$ Å
Volume	229.20(8) Å^3
Z	4
Density (calculated)	7.779 Mg/m^3
Radiation and wavelength	Mo$K\alpha$; $\lambda = 0.71073$ Å
Absorption coefficient, μ	38.841 mm^{-1}
$F(000)$	468
Crystal color	Metallic lustre
Crystal size	$0.23 \times 0.12 \times 0.09$ mm
Data collection	
Diffractometer	Enraf–Nonius Kappa CCD area-detector
θ range for data collection	$4.06^\circ \le \theta \le 30.07^\circ$
hkl range	$-10 \le h \le 10$; $-6 \le k \le 6$; $-9 \le l \le 9$
Measured reflections	1566
Absorption correction	Gaussian method
Independent reflections, R_{int} (obs/all)	372, 0.0927/0.0967
Refinement	
Refinement on	F^2
No. of independent reflections	372
No. of observed reflections ($I > 2\sigma(I)$)	291
No. of parameters	20
$R(F)$	0.0447
$wR(F^2)$	0.1024
S	1.28
Extinction coefficient	0.004(6)
Difference Fourier residues (e Å^{-3})	[+3.18, −3.06]

atoms appear to be strongly influenced by both size and electronegativity of the *RE* participating elements (13).

The crystallographic transformation with temperature presented by CeNiGa is similar to that observed recently for YbPdSn (14). This ternary stannide adopts at 870 K the hexagonal ZrNiAl-type structure and at 1400 K the orthorhombic TiNiSi-type structure. These two types derive from the well-known, simple aristotype AlB_2 (15). The polyhedra around the Ce-atoms in LTF and HTF CeNiGa are different. In LTF CeNiGa each Ce-atom has a sandwich-like coordination of four Ni- and six Ga-atoms in the form of two planar and parallel, ordered pentagons linked via a Ni-atom (Table 4). On the contrary, Ce-atom in HTF CeNiGa has six Ni- and six Ga-atoms in its coordination shell forming two strongly puckered and tilted hexagons. In other words, the chemical bond between Ce-atom and its ligands in the two crystallographic forms of CeNiGa may be different. It is interesting to note that this crystallographic transformation induces for YbPdSn a valence transition for ytterbium from trivalent state to divalent state (14).

The comparison of the structural properties of the two CeNiGa crystallographic forms indicates that: (i) the molar unit cell volume V_m of the LTF ($V_m = 55.53$ Å^3) is smaller than that of the HTF ($V_m = 57.30$ Å^3) polymorph; suggesting an increase of the hybridization strength of the $4f$(Ce) electrons with conduction electrons in the sequence HTF → LTF; (ii) V_m value of HTF is greater than that observed for CeNiAl ($V_m = 56.46$ Å^3) even though Ga presents an atomic radius smaller than that of Al (1); (iii) the smallest distances between Ce- and Ni-atoms are observed in

TABLE 2
Positional and Equivalent Isotropic Displacement Parameters U_{eq} (Å^2) for CeNiGa (HTF)

	x	y	z	U_{eq}
Ce	−0.02770(12)	$\frac{1}{4}$	0.67951(14)	0.0218(3)
Ni	0.1564(3)	$\frac{1}{4}$	0.0770(3)	0.0264(7)
Ga	0.3165(2)	$\frac{1}{4}$	0.3952(3)	0.0225(5)

TABLE 3
Anisotropic Displacement Parameters U^{ij} (Å^2) for CeNiGa (HTF)

	U^{11}	U^{22}	U^{33}	U^{12}	U^{13}	U^{23}
Ce	0.0195(5)	0.0158(6)	0.0300(5)	0	0.0000(4)	0
Ni	0.0291(11)	0.0198(13)	0.0302(12)	0	0.0003(8)	0
Ga	0.0193(8)	0.0161(10)	0.0322(10)	0	−0.0006(8)	0

TABLE 4
Selected Interatomic Distances in the Two CeNiGa Crystallographic Forms

Interatomic distances (Å)			
CeNiGa (LTF)[a]		CeNiGa (HTF)	
Ce–2 Ce	3.99(0)	Ce–2 Ce	3.355
−4 Ce	3.59(4)	−2 Ce	3.845
−4 Ga	3.24(9)	−Ga	3.115
−2 Ga	3.20(8)	−2 Ga	3.124
−Ni	2.94(3)	−2 Ga	3.165
−4 Ni	2.88(1)	−Ga	3.210
		−Ni	2.929
		−2 Ni	2.964
		−Ni	3.030
		−2 Ni	3.642

[a] Taken from Ref. (6).

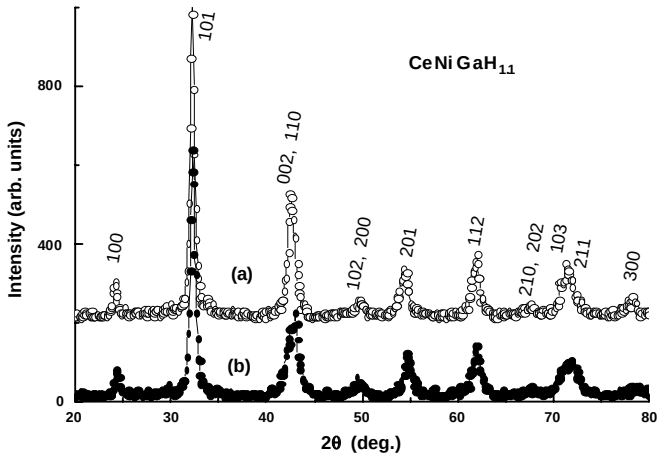

FIG. 2. X-ray powder pattern of hydride $CeNiGaH_{1.1}$ obtained from hydrogenation of CeNiGa (LTF) (a) and (HTF) (b).

CeNiGa (LTF) (Table 4). All these results suggest that the valence of cerium in CeNiGa depends strongly on the crystallographic form.

3.1.2. The Hydride $CeNiGaH_{1.1(1)}$

The two CeNiGa crystallographic forms absorb hydrogen at room temperature during the first exposure to a hydrogen pressure of 5 MPa. In both cases, the absorption results in formation of $CeNiGaH_{1.1(1)}$. No significant hydrogen desorption is observed during its heating up to 573 K under vacuum of 10^{-6} MPa indicating that the hydride is stable at least until this temperature. After synthesis, the hydride was handled in an Ar-filled glove box.

The hydrogenation induces a structural transition. $CeNiGaH_{1.1(1)}$ prepared from both CeNiGa (LTF) or (HTF) presents similar structural properties (Fig. 2). Its X-ray powder pattern is easily indexed on the basis of the hexagonal AlB_2-type structure (space group $P6/mmm$): Ce-atoms occupying the 1*a*-site (000), whereas Ni- and Ga-atoms being randomly distributed on the 2*d*-site ($\frac{1}{3}, \frac{2}{3}, \frac{1}{2}$). The refined unit cell parameters are $a = 4.239(4)$ Å and $c = 4.258(5)$ Å giving a molar volume of $V_m = 66.26$ Å^3. In other words, the hydrides $CeNiGaH_{1.1}$ and $CeNiAl_{1.93}$ are isomorphs (1).

The formation of CeNiGa hydride is accompanied by a large increase of the molar unit cell volume; respectively +19.3% and +15.6% after hydrogenation of LTF and HTF. The interatomic distances $d_{Ce-Ni,\ Ga}$ (12×3.244 Å) existing in $CeNiGaH_{1.1}$ are greater than those observed in both crystallographic forms of CeNiGa (Table 4). These steric considerations suggest that the valence state of the cerium could be modified during hydrogenation.

These results can be compared to those obtained recently by insertion of hydrogen in the ternary gallide CeIrGa (16). In this compound, hydrogenation induces a structural transition from orthorhombic TiNiSi-type to hexagonal Ni_2In-type which is a variant of the AlB_2-type with an ordering of the iridium and gallium atoms. In the present study, the atomic number of Ni and Ga is so close that X-ray powder diffraction does not show if similar ordering exists between Ni- and Ga-atoms in the hydride CeNi $GaH_{1.1}$. In order to solve this question an investigation of the hydride by neutron powder diffraction is needed.

3.2. Electrical Properties

Figure 3 shows the thermal dependence of the reduced electrical resistivity of the two CeNiGa forms (due to the presence of microcracks in the polycrystalline samples, absolute value of $\rho(T)$ could not be determined accurately; for this reason, reduced resistivity is reported). For CeNiGa (LTF), the reduced resistivity exhibits a quadratic temperature dependence between 4.2 and 70–75 K and then increases linearly with the temperature. This behavior characterizes a non-magnetic metal suggesting that the 4*f*(Ce) electrons are delocalized in CeNiGa (LTF). On the contrary, the resistivity of CeNiGa (HTF) presents a different temperature dependence: (i) an increase between 4.2 and 150 K showing a negative curvature; (ii) an almost constant value above 150 K. These observations are nearly similar to those reported for intermediate valence compounds based on cerium such as $CeIr_2Si_2$ (17), CeNiIn (18) or CeRhAl (19). The 4*f*-contribution of cerium to the resistivity of CeNiGa (HTF), obtained by subtracting the resistivity of CeNiGa (LTF) to the curve $\rho(T)/\rho(270\ \mathrm{K}) = f(T)$ relative to CeNiGa (HTF), shows a

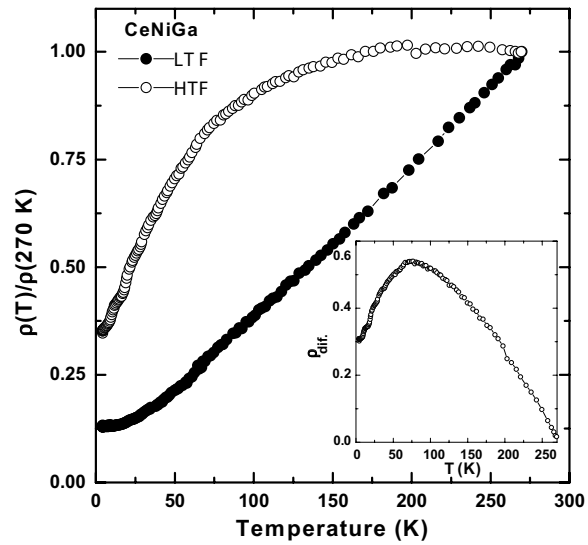

FIG. 3. Temperature dependence of the reduced electrical resistivity of the two CeNiGa forms. The inset shows the thermal dependence of the magnetic part of the resistivity of CeNiGa (HTF).

broad maximum centred around 75 K (inset of Fig. 3). Such behavior is typical of the intermediate valence cerium compounds (20). The occurrence of the broad maximum in the temperature dependence of the electrical resistivity is due to a spin-scattering mechanism in the intermediate valence regime.

The electrical resistivity measurements indicate that the spin-fluctuation temperature T_K (below which the hybridization between 4*f*(Ce)-electrons and conduction electrons occurs) of the CeNiGa (LTF) is much higher than that existing in CeNiGa (HTF).

3.3. Magnetic Properties

Figure 4 gives the thermal dependence of the magnetic susceptibility χ_m measured with an applied field $\mu_0 H = 4$ T for the two CeNiGa crystallographic forms.

Above 100 K, the magnetic susceptibility χ_m of CeNiGa (LTF) is practically independent of the temperature characterizing a Pauli paramagnet behavior. The increase of χ_m at low temperatures is mainly attributed to the presence of small amounts of stable moment Ce^{3+} ions from magnetic impurities such as Ce_2O_3. The $\chi_m = f(T)$ curve can be fitted according to $\chi_m = \chi_0 + nC/T$, where χ_0 is the temperature independent part of the susceptibility and n the proportion of stable Ce^{3+} moments ($C = 0.807$ emu K/mol) in the sample. This procedure gives $\chi_0 = 6.9 \times 10^{-3}$ emu/mol and $n = 22 \times 10^{-3}$. The absence of broad maximum in the curve $\chi_m = f(T)$ suggests that the spin−fluctuation temperature T_K is very high. This behavior is comparable to that observed for CeNiAl (1, 21), where the temperature T_K was estimated to be approximately 1000 K.

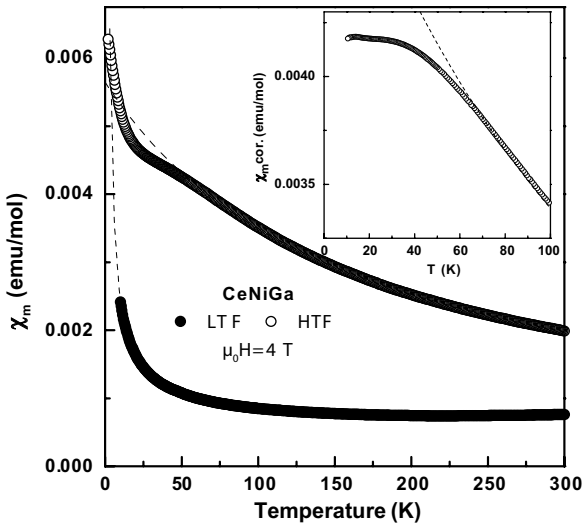

FIG. 4. Temperature dependence of the magnetic susceptibility of the two CeNiGa forms measured in a field of 4 T. The inset concerns the corrected magnetic susceptibility of CeNiGa (HTF).

The $\chi_m = f(T)$ curve relative to CeNiGa (HTF) reveals several features (Fig. 4): (i) above 100 K, the magnetic susceptibility follows a Curie–Weiss law $\chi_m = C/(T + \theta_p)$ where the Curie constant $C = 0.91$ emu K/mol ($\mu_{eff} = 2.70\,\mu_B$/mol) and the Curie paramagnetic temperature $\theta_p = -162$ K; these results indicate that in this temperature range cerium is trivalent; (ii) χ_m increases slowly between 60 and 20 K; (iii) below 20 K, χ_m exhibits a sharp increase with decreasing temperature due to a contribution of stable-moment Ce^{3+} situated in small amounts of impurity phase (this contribution is expressed by $\chi = nC/T$ where $C = 0.807$ emu K/mol and $n = 13 \times 10^{-3}$ deduced by the fitting again assuming Ce^{3+} impurities). The thermal dependence of the corrected magnetic susceptibility χ_m cor. (inset of Fig. 4), obtained by subtracting the impurity contribution, shows that this parameter ceases to depend on temperature below 40 K. This behavior can be ascribed to the existence of local spin fluctuations as a result of the occurrence of Kondo interactions or valence fluctuations. The large negative value of $\theta_p = -162$ K agrees well with this explanation. The observed thermal dependence of χ_m cor can be discussed in terms of a characteristic temperature T_K related to Kondo-type fluctuations (22). In this scheme, T_K is defined at low temperatures as $T_K = C/2\chi(0)$ where $C = 0.807$ emu K/mol is the Curie constant and $\chi(0) = 4.22 \times 10^{-3}$ emu/mol the magnetic susceptibility at $T = 0$ K. In these conditions T_K is estimated to be 95(5) K.

The evolution of Kondo temperature T_K CeNiGa (LTF) $\gg T_K$ CeNiGa (HTF) shows that the mixing between 4*f*(Ce) and the conduction band states is more pronounced in the first crystallographic form. This fact which agrees with the results deduced from the electrical resistivity measurements is certainly due to a broadening of the conduction band induced by a decrease of the molar unit cell volume V_m in the sequence CeNiGa (HTF) → CeNiGa (LTF). From the study of the magnetic properties of CeNiGa, Grin *et al.* (7) claim also that Ce^{3+} is present in CeNiGa (HTF). But in this last work, performed by magnetic measurements only above 80 K, no spin fluctuation temperature T_K was determined.

Figure 5 compares the temperature dependence of the reciprocal magnetic susceptibility χ_m of ternary gallide CeNiGa (HTF) and its hydride $CeNiGaH_{1.1}$. Below 300 K, the susceptibility of hydride is higher than that of gallide. Above 100 K, the data relative to $CeNiGaH_{1.1}$ can be fitted with a Curie–Weiss law $\chi_m^{-1} = (T - \theta_p)/C_m$ giving $\theta_p = -100$ K and $\mu_{eff} = (8C_m/3)^{\frac{1}{2}} = 2.52\,\mu_B$/Ce. The effective moment value is very close to that calculated for a free Ce^{3+} ion (2.54 μ_B). The negative curvature observed at low temperatures in the $\chi_m^{-1} = f(T)$ curve, indicates the presence of a crystal-field effect. The broad minimum appearing in the temperature range 60–20 K in the $\chi_m^{-1} = f(T)$ curve relative to CeNiGa (HTF) is not detected for

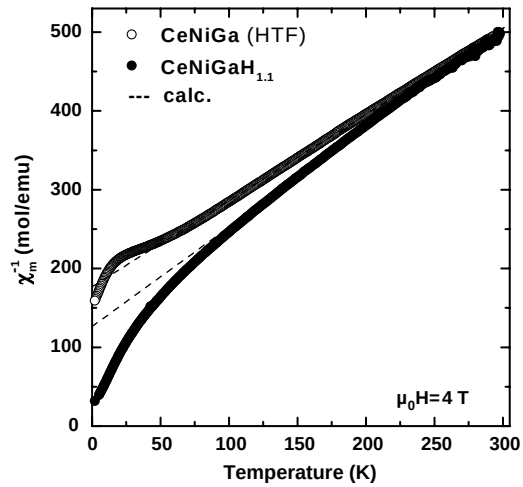

FIG. 5. Temperature dependence of the reciprocal magnetic susceptibility, measured with an applied field $\mu_0 H = 4\,T$, of gallide CeNiGa (HTF) and hydride $CeNiGaH_{1.1}$.

the hydride. In other words, hydrogenation of this ternary gallide induces a change of the valence state of cerium from intermediate to purely trivalent. Moreover, unlike $CeNiAlH_{1.93}$ which shows a spin fluctuation behavior below 7 K (1), the hydride $CeNiGaH_{1.1}$ presents above 1.8 K neither signature of the occurrence of Kondo temperature nor magnetic ordering temperature. This hydride may be a "heavy fermion" compound. In order to solve this question, heat capacity measurements are necessary.

4. CONCLUSION

The hydrogenation of the two CeNiGa crystallographic forms (LTF and HTF) leads, as for CeNiAl (1), to a structural transition from hexagonal ZrNiAl-type (LTF) or orthorhombic TiNiSi-type (HTF) to hexagonal AlB_2-type. This behavior is significantly different from that observed during the hydrogenation of similar indide CeNiIn; the hydride $CeNiInH_{1.6-1.8}$ adopts the same structure type (hexagonal ZrNiAl) as that of CeNiIn (3, 4). The possible sites for insertion of the H-atom in CeNiAl or CeNiGa are too small and implies the structural transition.

The valence state of the cerium in CeNiGa and its hydride are very different. CeNiGa (LTF) and (HTF) are considered as intermediate valence compounds having, respectively, $T_K \gg 300\,K$ and $T_K \cong 95(5)\,K$ as Kondo temperature, whereas $CeNiGaH_{1.1}$ is based on purely trivalent cerium. The valence transition occurring by hydrogenation is correlated to a strong increase of the molar unit cell volume. The insertion of hydrogen in intermetalics based on cerium induces a decrease of the Kondo interaction. The recent works devoted to the hydrogenation of CeNiAl (1), CeIrAl (23), CeIrGa (16) and CeNiGa (this work) agree with this hypothesis; in all cases the hydrogenation induces a localization of the 4*f*(Ce)-electron. Now, it is interesting to perform similar experiments on other intermediate valence compounds in order to find a hydride showing magnetic ordering.

ACKNOWLEDGMENTS

The authors would like to thank Mr. R. Decourt for his technical assistance during the electrical resistivity measurements.

REFERENCES

1. J.-L. Bobet, B. Chevalier, B. Darriet, M. Nakhl, F. Weill, and J. Etourneau, *J. Alloys Compol.* **317–318,** 67 (2001).
2. K. Ghoshray, B. Bandyopadhyay, Mita Sen, A. Ghoshray, and N. Chatterjee, *Phys. Rev. B* **47,** 8277 (1993).
3. Mita Sen, Saurav Giri, K. Ghoshray, B. Bandyopadhyay, A. Ghoshray, and N. Chatterjee, *Solid State Commun.* **89,** 327 (1994).
4. I. I. Bulyk, V. A. Yartys, R. V. Denys, Ya. M. Kalychak, and I. R. Harris, *J. Alloys Compd.* **284,** 256 (1999).
5. J. P. Kuang, H. J. Cui, J. Y.Li, F. M. Yang, H. Nakotte, E. Brück, and F. R. de Boer, *J. Magn. Magn. Mater.* **104–107,** 1475 (1992).
6. Yu. P. Yarmolyuk, Yu. N. Gryn, and E. I. Gladyshevsky, Dopov. *Akad. Nauk. Ukr. RSR, Ser. A* **9,** 771 (1979).
7. Yu. N. Grin, K. Hiebl, and P. Rogl, *J. Less-Comm. Metals* **110,** 299 (1985).
8. J.-L. Bobet, S. Pechev, B. Chevalier, and B. Darriet, *J. Alloys Compd.* **267,** 136 (1998).
9. J. Rodriguez-Carvajal, Powder diffraction, *in*: "Satellite Meeting of the 15th Congress of IUCr," Toulouse, p. 127. 1990.
10. V. Petricek and M. Dusek, "The Crystallographic Computing System Jana 2000." Institute of Physics, Praha, Czech Republic.
11. G. M. Sheldrick, "SHELXS-97. Crystal structure solution." University of Göttingen, Germany, 1997.
12. P. J. Becker and P. Coppens, *Acta Crystallogr. A* **30,** 129 (1974).
13. E. Hovestreydt, N. Engel, K. Klepp, B. Chabot, and E. Parthé, *J. Less-Comm. Metals* **85,** 247 (1982).
14. D. Kubmann, R. Pöttgen, B. Künnen, G. Kotzyba, R. Müllmann, and B. D. Mosel, *Z. Kristallogr.* **213,** 356 (1998).
15. R. D. Hoffmann and R. Pöttgen, *Z. Kristallogr.* **216,** 127 (2001).
16. P. Raj, A. Sathyamoorthy, K. Shashikala, C. R. Venkateswara Rao, and S. K. Malik, *Solid State Commun* **120,** 375 (2001).
17. B. Buffat, B. Chevalier, M. H. Tuilier, B. Lloret, and J. Etourneau, *Solid State Commun.* **99,** 17 (1986).
18. H. Fujii, T. Inoue, Y. Andoh, T. Takabatake, K. Satoh, Y. Maeno, T. Fujita, J. Sakurai, and Y. Yamaguchi, *Phys. Rev. B* **39,** 6840 (1989).
19. N. Harish Kumar and S. K. Malik, *Phys. Rev. B* **62,** 127 (2000).
20. W. H. Lee, H. C. Ku, and R. N. Shelton, *Phys. Rev. B* **36,** 5739 (1987).
21. L. Menon, A. Agarwal, and S. K. Malik, *Physica B* **230–232,** 201 (1997).
22. J. M. Lawrence, P. S. Riseborough, and R. D. Parks, *Rep. Prog. Phys.* **44,** 1 (1981).
23. S. K. Malik, P. Raj, A. Sathyamoorthy, K. Shashikala, N. Harish Kumar, and Latika Menon, *Phys. Rev. B* **63,** 172418 (2001).